Role of A$_{2B}$ adenosine receptor signaling in adenosine-dependent pulmonary inflammation and injury

Chun-Xiao Sun, … , Dewan Zeng, Michael R. Blackburn

Research Article   **Pulmonology**

Adenosine has been implicated in the pathogenesis of chronic lung diseases such as asthma and chronic obstructive pulmonary disease. In vitro studies suggest that activation of the A$_{2B}$ adenosine receptor (A$_{2B}$AR) results in proinflammatory and profibrotic effects relevant to the progression of lung diseases; however, in vivo data supporting these observations are lacking. Adenosine deaminase–deficient (ADA-deficient) mice develop pulmonary inflammation and injury that are dependent on increased lung adenosine levels. To investigate the role of the A$_{2B}$AR in vivo, ADA-deficient mice were treated with the selective A$_{2B}$AR antagonist CVT-6883, and pulmonary inflammation, fibrosis, and airspace integrity were assessed. Untreated and vehicle-treated ADA-deficient mice developed pulmonary inflammation, fibrosis, and enlargement of alveolar airspaces; conversely, CVT-6883–treated ADA-deficient mice showed less pulmonary inflammation, fibrosis, and alveolar airspace enlargement. A$_{2B}$AR antagonism significantly reduced elevations in proinflammatory cytokines and chemokines as well as mediators of fibrosis and airway destruction. In addition, treatment with CVT-6883 attenuated pulmonary inflammation and fibrosis in wild-type mice subjected to bleomycin-induced lung injury. These findings suggest that A$_{2B}$AR signaling influences pathways critical for pulmonary inflammation and injury in vivo. Thus in chronic lung diseases associated with increased adenosine, antagonism of A$_{2B}$AR-mediated responses may prove to be a beneficial therapy.

Find the latest version:

https://jci.me/27303/pdf

Role of A$_{2B}$ adenosine receptor signaling in adenosine-dependent pulmonary inflammation and injury

Chun-Xiao Sun,[1] Hongyan Zhong,[2] Amir Mohsenin,[1] Eva Morschl,[1] Janci L. Chunn,[1] Jose G. Molina,[1] Luiz Belardinelli,[2] Dewan Zeng,[2] and Michael R. Blackburn[1]

[1]Department of Biochemistry and Molecular Biology, University of Texas Medical School at Houston, Houston, Texas, USA.
[2]Department of Drug Research and Pharmacological Sciences, CV Therapeutics Inc., Palo Alto, California, USA.

Adenosine has been implicated in the pathogenesis of chronic lung diseases such as asthma and chronic obstructive pulmonary disease. In vitro studies suggest that activation of the A$_{2B}$ adenosine receptor (A$_{2B}$AR) results in proinflammatory and profibrotic effects relevant to the progression of lung diseases; however, in vivo data supporting these observations are lacking. Adenosine deaminase–deficient (ADA-deficient) mice develop pulmonary inflammation and injury that are dependent on increased lung adenosine levels. To investigate the role of the A$_{2B}$AR in vivo, ADA-deficient mice were treated with the selective A$_{2B}$AR antagonist CVT-6883, and pulmonary inflammation, fibrosis, and airspace integrity were assessed. Untreated and vehicle-treated ADA-deficient mice developed pulmonary inflammation, fibrosis, and enlargement of alveolar airspaces; conversely, CVT-6883–treated ADA-deficient mice showed less pulmonary inflammation, fibrosis, and alveolar airspace enlargement. A$_{2B}$AR antagonism significantly reduced elevations in proinflammatory cytokines and chemokines as well as mediators of fibrosis and airway destruction. In addition, treatment with CVT-6883 attenuated pulmonary inflammation and fibrosis in wild-type mice subjected to bleomycin-induced lung injury. These findings suggest that A$_{2B}$AR signaling influences pathways critical for pulmonary inflammation and injury in vivo. Thus in chronic lung diseases associated with increased adenosine, antagonism of A$_{2B}$AR-mediated responses may prove to be a beneficial therapy.

Introduction

Lung inflammation, tissue remodeling, and airway destruction are noted features of various chronic pulmonary diseases. Pulmonary infiltration with lymphocytes and eosinophils together with mucus hypersecretion and airway remodeling are characteristics of asthma (1). In contrast, chronic obstructive pulmonary disease (COPD) is associated with largely monocytic inflammation and destruction of alveolar airways (2), while interstitial lung diseases such as usual and desquamative interstitial pneumonias exhibit varying degrees of inflammation and airway fibrosis (3). Although each of these lung pathologies has unique inflammatory and structural changes, they share the common feature of being chronic in nature. For example, the lung tissue alterations seen in these diseases are not readily resolvable and progress with disease exacerbations. Substantial information is available describing how cytokines, growth factors, and protease/antiprotease imbalances can lead to the inflammation and damage of the lungs (1, 3–5). However, little is known about the signaling pathways that drive the progressive inflammation and tissue remodeling/destruction. Identifying pathways that are activated in response to injury in the lung may provide insight into novel approaches to treat ongoing chronic lung diseases.

Adenosine is a signaling molecule that is generated at sites of tissue injury and inflammation. Consistent with this, adenosine levels are elevated in the circulation during sepsis (6) and in tissues following ischemia (7). Adenosine levels are also elevated in the bronchial alveolar lavage (BAL) fluid (8) and exhaled breath condensate of asthmatics (9), where the magnitude of adenosine formed correlates with the magnitude of pulmonary inflammation (9). Studies in animal models have revealed that adenosine can have vastly different effects on the regulation of inflammation and tissue injury. Adenosine has potent antiinflammatory and tissue protective effects in acute injury processes such as those seen in ischemia/reperfusion injury (10) and responses to endotoxin (11). In contrast, increased levels of adenosine in chronic inflammation and injury models can activate proinflammatory and tissue destructive pathways (12). Mice that overexpress the Th2 cytokine IL-13 in the lung develop chronic pulmonary inflammation, fibrosis, and enlargement of alveolar airspaces in association with increased tissue levels of adenosine (13). Treatment of these mice with adenosine deaminase (ADA), which metabolizes adenosine, lowers lung adenosine levels and leads to decreased inflammation and fibrosis as well as enlargement of alveolar airspaces (13), suggesting that adenosine can activate pathways that play a role in the pathophysiology of chronic lung disease. This hypothesis is supported further by findings in mice genetically deficient in ADA. ADA-deficient mice spontaneously develop severe pulmonary inflammation, airway remodeling, fibrosis, and enlargement of airspaces in association with increases in adenosine levels in lung tissue (14–16). Thus increases in endogenous adenosine levels can promote pathophysiological features seen in chronic lung diseases. However, the specific pathways involved in these processes are not yet known.

Adenosine elicits its actions on cells by activating cell surface G protein–coupled adenosine receptors (ARs). Four distinct ARs
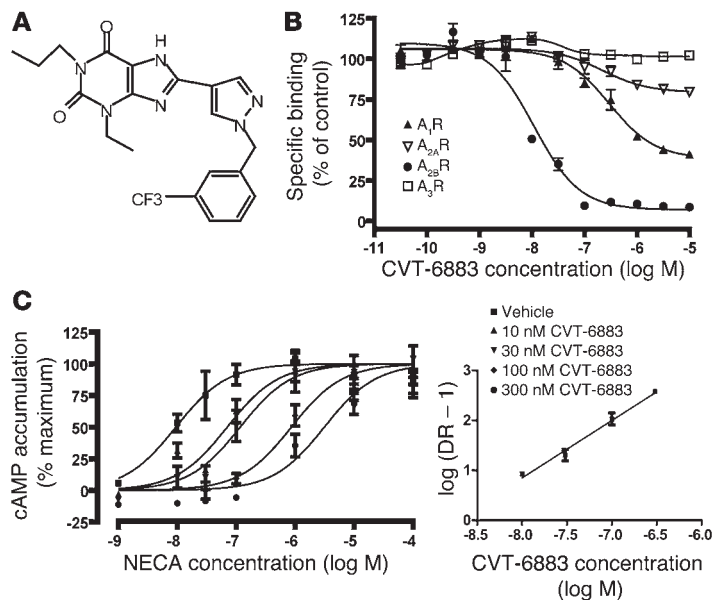
Figure 1

Pharmacological characterization of CVT-6883 as an $A_{2B}AR$ antagonist. (**A**) Structure of CVT-6883. (**B**) Competition of CVT-6883 for specific radioligand binding to membranes prepared from CHO cells overexpressing the A_1AR or A_3AR or from HEK cells over-expressing the $A_{2A}AR$ or $A_{2B}AR$. Increasing concentrations of CVT-6883 were used to displace the specific binding of selective receptor radioligands: ^{3}H-CPX (A_1AR antagonist; 0.45 nM), ^{3}H-ZM241385 ($A_{2A}AR$ antagonist; 1.6 nM), ^{3}H-ZM241385 ($A_{2B}AR$ antagonist; 9.3 nM), or ^{3}H-MRE3008F20 (A_3AR antagonist; 0.63 nM). Data are presented as mean ± SEM percent specific binding of control from 6 determinations. (**C**) Concentration response curves of NECA-induced increases in cAMP in the absence or presence of increasing concentrations of CVT-6883. Mouse NIH/3T3 cells were treated with NECA (1 nM to 100 μM) in the absence or presence of increasing concentrations of CVT-6883, and cAMP accumulation was measured. Data are mean ± SEM from 3 experiments performed in duplicate. Inset is the Schild plot. DR – 1, concentration ratio minus 1.

are present in mammalian cells: A_1AR, $A_{2A}AR$, $A_{2B}AR$, and A_3AR (17). These receptors have differing affinities for adenosine and adenosine analogs, and their patterns and levels of expression on cells are diverse and variable, respectively. Genetic and pharmacologic approaches have been used to determine the contribution of ARs to the adenosine-dependent pulmonary inflammation and damage seen in ADA-deficient mice. Genetic removal of the high-affinity A_1AR from ADA-deficient mice leads to an exacerbation in pulmonary inflammation and damage, suggesting that this receptor plays an antiinflammatory and protective role in this model (16). In contrast, pharmacologic blockade or genetic removal of the A_3AR can diminish certain aspects of pulmonary inflammation in the lungs of ADA-deficient mice, including mast cell degranulation and eosinophilia (18, 19). The contribution of the $A_{2A}AR$ and the $A_{2B}AR$ in this model has not yet been examined. These findings demonstrate that AR signaling plays important roles in the regulation of lung inflammation and remodeling in ADA-deficient mice.

Of the 4 receptors, the $A_{2B}AR$ has the lowest affinity for adenosine (20, 21) and may only be stimulated in situations where adenosine levels are increased. In addition, activation of the $A_{2B}AR$ can promote the differentiation of pulmonary fibroblasts into myofibroblasts (22) and can stimulate the expression of mediators from various cells implicated in the regulation of pulmonary inflammation and remodeling (23–25). Furthermore, there is increased expression of the $A_{2B}AR$ in the lungs of ADA-deficient mice in association with increased tissue levels of adenosine and marked pulmonary inflammation and injury (26). These findings led us to hypothesize that the $A_{2B}AR$ may contribute to the proinflammatory and tissue-destructive effects of adenosine in the lung. To test this hypothesis, we used what we believe to be a newly developed $A_{2B}AR$ antagonist to determine the contribution of $A_{2B}AR$ signaling to the adenosine-dependent pulmonary inflammation and injury seen in ADA-deficient mice. Our results demonstrated that $A_{2B}AR$ antagonism can prevent the development of pulmonary inflammation, airspace enlargement, and airway fibrosis in the lungs of ADA-deficient mice. In addition, $A_{2B}AR$ antagonism led to decreased expression of key cytokines, chemokines, and proteases

in the lung. $A_{2B}AR$ antagonism also attenuated bleomycin-induced pulmonary injury in wild-type mice. These findings implicate the $A_{2B}AR$ as a major mediator of chronic lung disease and suggest that antagonists against this receptor may have important utility in the treatment of certain pulmonary diseases.

Results

CVT-6883 is a selective $A_{2B}AR$ antagonist. The novel compound CVT-6883 (Figure 1A) was synthesized, and its binding affinity for the 4 subtypes of ARs was determined using competition radioligand binding assays in membranes isolated from cell lines that overexpress each of the 4 human ARs (Figure 1B). The calculated K_I value
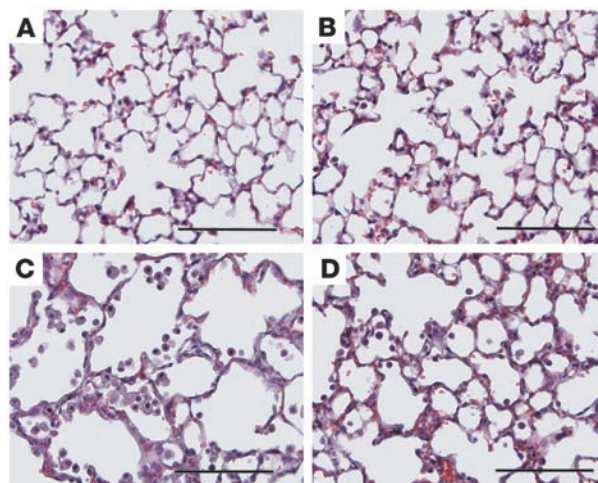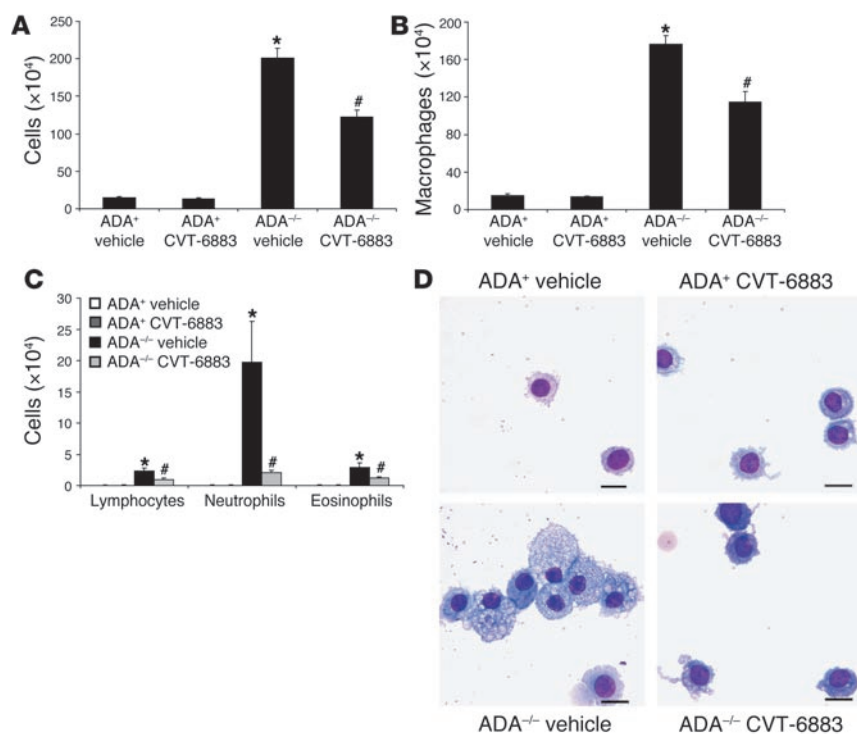

Figure 2

Histopathology of the lungs of mice treated with CVT-6883. Lungs were collected from postnatal day 38 mice and prepared routinely for sectioning and H&E staining. (**A**) Lung from an *ADA+* mouse treated with vehicle. (**B**) Lung from an *ADA+* mouse treated with CVT-6883. (**C**) Lung from an *ADA−/−* mouse treated with vehicle. (**D**) Lung from an *ADA−/−* mouse treated with CVT-6883. Sections are representative of 6–8 different mice from each treatment group. Scale bars: 100 μm.

Figure 3
Airway inflammatory cells in mice treated with CVT-6883. (**A**) BAL fluid was collected from postnatal day 38 mice, and total cell numbers were counted. (**B** and **C**) BAL cells were cyto-spun and stained with Diff-Quick, allowing for determination of cellular differentials. Data are mean cell counts ± SEM. *$P \leq 0.05$ versus vehicle-treated ADA^+ mice; #$P \leq 0.05$ versus vehicle-treated $ADA^{-/-}$ mice. $n = 8$ (ADA^+), 6–8 ($ADA^{-/-}$). (**D**) Increased numbers of foam cells were found by directly examining cytospun cells stained with Diff-Quick. Scale bars: 10 μm.

(affinity) of CVT-6883 for the $A_{2B}AR$ was 8.3 ± 2.6 nM. CVT-6883 (10 μM) caused 59% ± 4% and 20% ± 4% reductions in the specific radioligand binding to the A_1AR and the $A_{2A}AR$, respectively. However, 10 μM CVT-6883 did not significantly reduce the radioligand binding to the A_3AR. These findings demonstrate that CVT-6883 has a much greater affinity for the $A_{2B}AR$ than the other ARs.

Activation of the $A_{2B}AR$ leads to increases in cAMP concentrations (17). To determine the ability of CVT-6883 to function as an $A_{2B}AR$ antagonist, the potencies of CVT-6883 in inhibiting agonist-stimulated elevations in cAMP were determined. CVT-6883 caused a rightward shift in the concentration response curve for the $A_{2B}AR$ agonist 5′(N-ethylcarboxamido)adenosine (NECA) (Figure 1C). The calculated K_B (binding potency) value for CVT-6883 at the mouse $A_{2B}AR$ was 2.2 ± 0.8 nM, indicating that CVT-6883 is a potent antagonist of NECA-stimulated increases in cAMP mediated by the mouse $A_{2B}AR$. Similar findings were found using HEK-293 cells expressing human $A_{2B}ARs$ (data not shown), which suggests that CVT-6883 is also a potent antagonist of the human $A_{2B}AR$. CVT-6883 (10 μM) showed no significant effect on other common receptors, ion channels, transporters, and enzymes (data not shown). Collectively, these data demonstrate that CVT-6883 is a high-affinity, selective $A_{2B}AR$ antagonist and a specific adenosine antagonist.

Inhibition of pulmonary inflammation following treatment with CVT-6883. ADA-deficient ($ADA^{-/-}$) mice develop pulmonary insufficiencies associated in part with progressive pulmonary inflammation, which is characterized by increases in activated alveolar macrophages, lymphocytes, neutrophils, and eosinophils (14). To determine the involvement of $A_{2B}AR$ signaling in the pulmonary phenotypes seen in $ADA^{-/-}$ mice, animals were treated with CVT-6883. In all experiments, $ADA^{-/-}$ mice were maintained on ADA enzyme therapy from birth to postnatal day 21 to prevent defects in alveolar development (27). ADA enzyme therapy was discontinued at postnatal day 21, and 3 days later mice were given intraperitoneal injections of 1 mg/kg

CVT-6883 twice daily for 14 days. All pulmonary end points were examined at the end of this treatment regimen (postnatal day 38). Controls were either untreated mice or mice treated with vehicle alone. At the termination of the experiment, plasma levels of CVT-6883 reached average concentrations of 933 ± 99 ng/ml (2 μM), while concentrations in the BAL fluid were 18 ± 7 ng/ml (40 nM). Findings in Figure 1 suggest that these levels are sufficient for $A_{2B}AR$ antagonism but are below levels capable of antagonism of other ARs.

Histological analysis of lungs from mice treated according to the above protocol is shown in Figure 2. The lungs of $ADA^{-/-}$ mice treated with vehicle exhibited increased pulmonary inflammation (Figure 2C), findings identical to those seen in untreated $ADA^{-/-}$ mice (data not shown). Treatment with CVT-6883 did not affect the histopathology of the lungs of control ADA^+ mice (Figure 2B), but it caused decreased inflammation in the lungs of $ADA^{-/-}$ mice (Figure 2D). These findings were quantified by counting inflammatory cells recovered from BAL fluid (Figure 3). Results revealed a significant reduction in the number of total cells recovered from BAL fluid of $ADA^{-/-}$ mice treated with CVT-6883 compared with vehicle-treated $ADA^{-/-}$ mice (Figure 3A). Analysis of cellular differentials from the BAL fluid revealed a reduction in all cell types examined, including alveolar macrophages (Figure 3B) and lymphocytes, neutrophils, and eosinophils (Figure 3C). Examination of alveolar macrophages demonstrated that macrophages recovered from the lungs of vehicle-treated $ADA^{-/-}$ mice were enlarged and foamy, whereas those recovered from the BAL of CVT-6883–treated $ADA^{-/-}$ mice were not (Figure 3D). These data demonstrate a significant decrease in airway inflammation in $ADA^{-/-}$ mice treated with CVT-6883, suggesting that $A_{2B}AR$ antagonism can attenuate airway inflammation in this model.

Reduction in cytokine levels in the lungs of CVT-6883–treated mice. The ability of CVT-6883 treatment to dampen pulmonary inflammation in $ADA^{-/-}$ mice prompted us to determine the levels of rel-
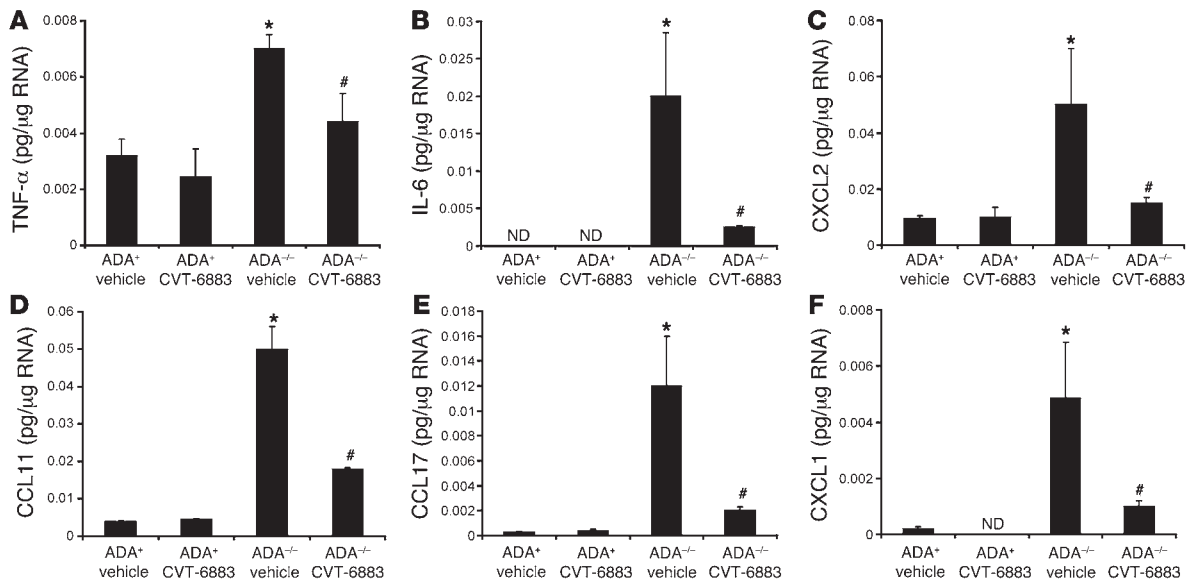
Figure 4
Production of proinflammatory cytokines. Transcript levels of various proinflammatory cytokines were measured in whole-lung extracts from postnatal day 38 mice using quantitative RT-PCR. Shown are levels of (**A**) TNF-α, (**B**) IL-6, (**C**) CXCL2, (**D**) CCL11, (**E**) CCL17, and (**F**) CXCL1. Results are presented as mean pg transcript/μg RNA ± SEM. *$P \leq 0.05$ versus vehicle-treated *ADA+* mice; #$P \leq 0.05$ versus vehicle-treated *ADA−/−* mice. $n = 4$ (*ADA+*), 8 (*ADA−/−*). ND, not detected.

evant cytokines and chemokines. Whole-lung RNA extracts from *ADA+* and *ADA−/−* mice treated with vehicle or CVT-6883 were analyzed. Expression of IL-5, IL-4, RANTES, and various monocyte chemoattractant proteins was found to be increased in the lungs of *ADA−/−* mice treated with vehicle; however, their expression did not change with CVT-6883 treatment (data not shown). In contrast, expression of TNF-α, IL-6, CCL11 (eotaxin I), CCL17 (TARC), CXCL1 (groα), and CXCL2 (groβ) was increased in vehicle-treated *ADA−/−* mice and significantly lower in *ADA−/−* mice treated with CVT-6883 (Figure 4). These findings demonstrate that A$_{2B}$AR antagonism in *ADA−/−* mice is able to inhibit the expression of certain proinflammatory cytokines and chemokines.

Inhibition of alveolar airspace enlargement following CVT-6883 treatment. *ADA−/−* mice develop features of alveolar airspace enlargement that are characteristic of emphysema (14, 16). To determine the effect of CVT-6883 on the enlargement of airspaces in *ADA−/−* mice, alveolar airspace size was measured histologically by determining mean chord length of airspaces (Figure 5). The airspaces of *ADA+* animals were well ordered when viewed histologically (Figure 5, A and B), whereas airspaces from vehicle-treated *ADA−/−* mice were enlarged (Figure 5C). Treatment of *ADA−/−* mice with CVT-

6883 prevented this enlargement (Figure 5D). Results of quantification of alveolar airspace size were consistent with the histological observations (Figure 5E), demonstrating that treatment of *ADA−/−* mice with CVT-6883 inhibits alveolar airway destruction.
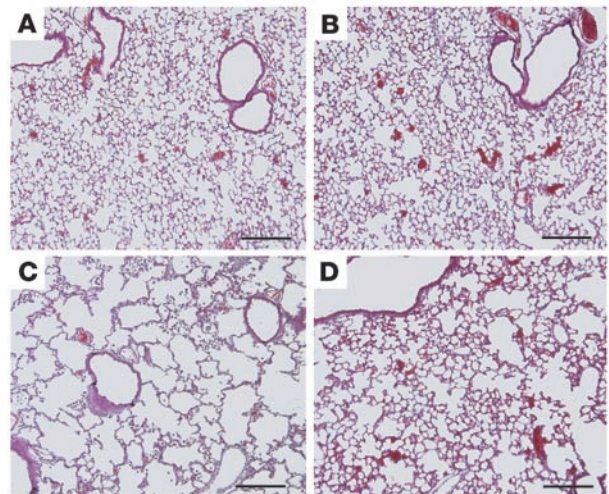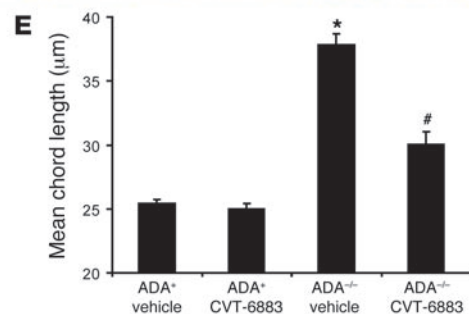

Figure 5
CVT-6883 treatment inhibits alveolar airway enlargement in *ADA−/−* mice. Lungs from postnatal day 38 mice were infused with fixative under constant pressure (25 cm H$_2$O) and processed for H&E staining. (**A**) Lung from an *ADA+* mouse treated with vehicle. (**B**) Lung from an *ADA+* mouse treated with CVT-6883. (**C**) Lung from an *ADA−/−* mouse treated with vehicle. (**D**) Lung from an *ADA−/−* mouse treated with CVT-6883. Images are representative of 8 animals from each group. Scale bars: 100 μm. (**E**) Alveolar airspace size was calculated using Image-Pro analysis software; data are mean chord length ± SEM. *$P \leq 0.05$ versus vehicle-treated *ADA+* mice; #$P \leq 0.05$ versus vehicle-treated *ADA−/−* mice. $n = 5$ per group.
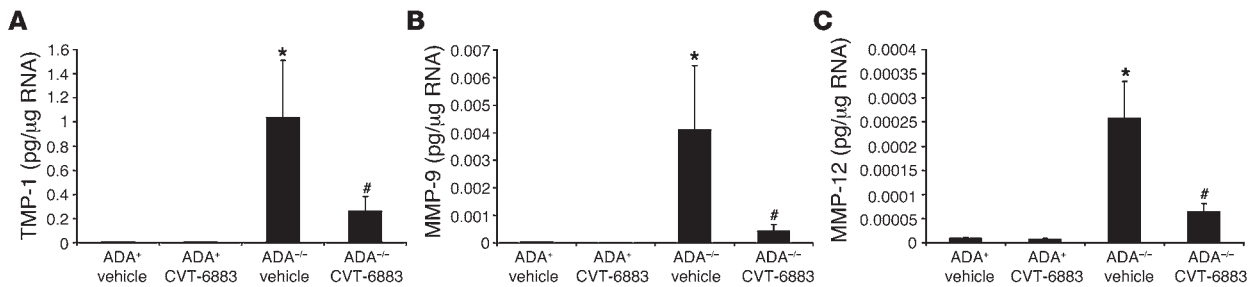
Figure 6
CVT-6883 treatment inhibits the expression of genes associated with alveolar airway destruction. Transcript levels of TIMP-1 (**A**), MMP-9 (**B**), and MMP-12 (**C**) were measured in whole-lung RNA extracts from postnatal day 38 mice using quantitative RT-PCR. Data are mean pg transcript/μg RNA ± SEM. *$P \leq 0.05$ versus vehicle-treated ADA^+ mice; #$P \leq 0.05$ versus vehicle-treated $ADA^{-/-}$ mice. $n = 4$ (ADA^+), 8 ($ADA^{-/-}$).

Normalization of protease/antiprotease levels in the lungs of CVT-6883–treated mice. Increased levels of MMPs and inhibitors of proteases are features of alveolar airspace enlargement in many models including $ADA^{-/-}$ mice (16, 28, 29). Measurement of antiproteases and proteases in the lungs of $ADA^{-/-}$ mice treated with vehicle demonstrated an increase in the expression of tissue inhibitor of metalloproteinase–1 (TIMP-1), MMP-9, and MMP-12 (Figure 6). Treatment of $ADA^{-/-}$ mice with CVT-6883 led to diminished expression of all 3 of these regulators of alveolar integrity, suggesting that $A_{2B}AR$ signaling is involved in regulating adenosine-induced protease and antiprotease expression in the lungs of $ADA^{-/-}$ mice.

Treatment with CVT-6883 results in decreased pulmonary fibrosis. Previous studies have demonstrated that $ADA^{-/-}$ mice develop pulmonary fibrosis in conjunction with increases in tissue levels of adenosine (15). To determine the effect of CVT-6883 treatment on pulmonary fibrosis in $ADA^{-/-}$ mice, the status of pulmonary myofibroblasts was examined by staining for α-SMA (Figure 7, A–C). No α-SMA–positive cells were

seen in the distal airways of ADA^+ vehicle-treated mice (Figure 7A), whereas α-SMA staining was prominent in the distal airways of vehicle-treated $ADA^{-/-}$ mice (Figure 7B). Few to no α-SMA–positive cells were seen in the alveolar airways of $ADA^{-/-}$ mice treated with CVT-6883 (Figure 7C), suggesting that $A_{2B}AR$ antagonism inhibits the accumulation of myofibroblasts in the lungs of $ADA^{-/-}$ mice.
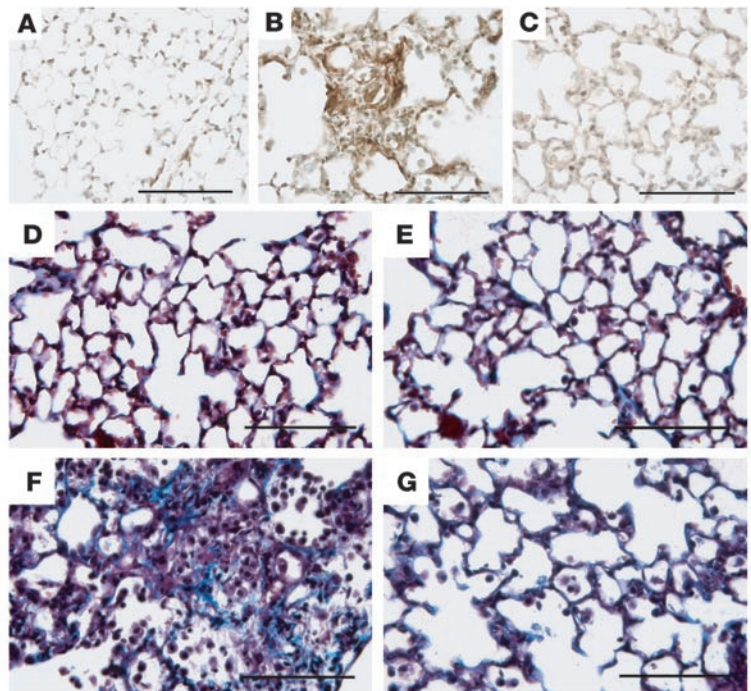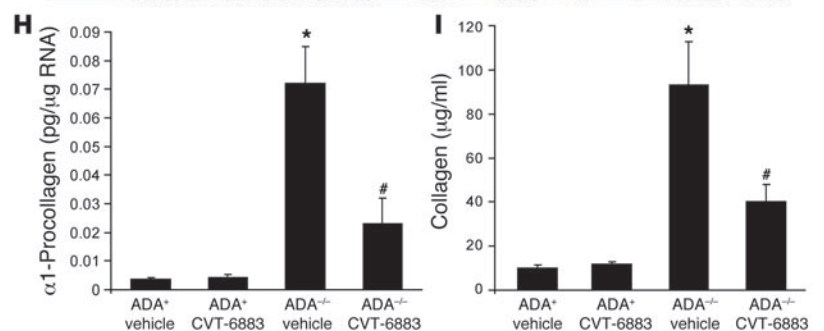

Figure 7
Pulmonary fibrosis in $ADA^{-/-}$ mice treated with CVT-6883. (**A–C**) Lung sections from postnatal day 38 mice were stained with an antibody against α-SMA to visualize myofibroblast (brown stain). (**A**) Lung from an ADA^+ mouse treated with vehicle. (**B**) Lung from an $ADA^{-/-}$ mouse treated with vehicle. (**C**) Lung from an $ADA^{-/-}$ mouse treated with CVT-6883. (**D–F**) Lung sections were stained with Masson's trichrome to visualize collagen deposition (blue stain). (**D**) Lung from an ADA^+ mouse treated with vehicle. (**E**) Lung from an ADA^+ mouse treated with CVT-6883. (**F**) Lung from an $ADA^{-/-}$ mouse treated with vehicle. (**G**) Lung from an $ADA^{-/-}$ mouse treated with CVT-6883. Sections are representative of 6 different mice from each treatment. Scale bars: 100 μm. (**H**) Whole-lung α1-procollagen transcript levels. Data are mean pg transcript/μg RNA ± SEM. (**I**) Soluble collagen protein levels. Data are mean μg collagen/ml BAL fluid ± SEM. *$P \leq 0.05$ versus vehicle-treated ADA^+; #$P \leq 0.05$ versus vehicle-treated $ADA^{-/-}$. $n = 4$ (ADA^+), 8 ($ADA^{-/-}$).
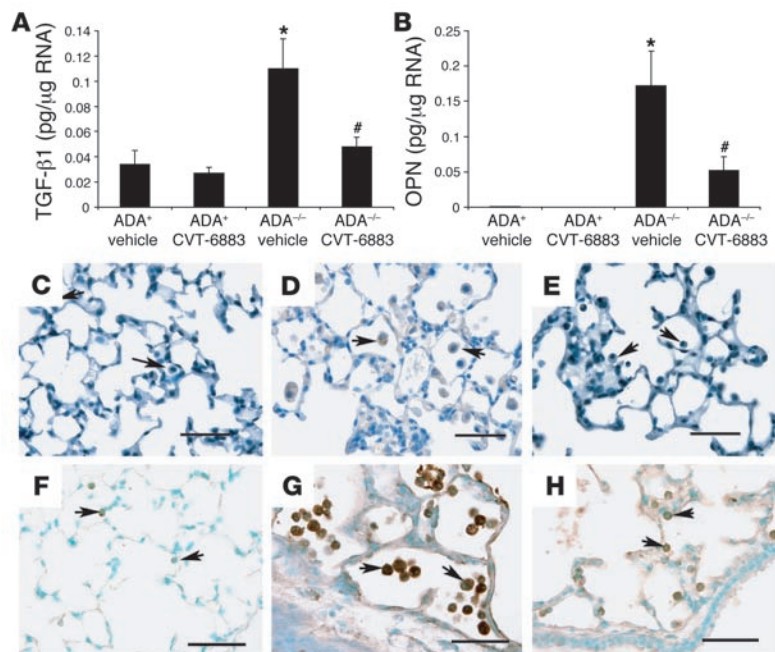
Figure 8
CVT-6883–treated $ADA^{-/-}$ mice had decreased expression of TGF-β1 and OPN in alveolar macrophages. RNA was extracted from whole lungs of postnatal day 38 mice for analysis using quantitative RT-PCR for various fibrosis-associated transcripts. Results demonstrate that lungs from CVT-6883–treated $ADA^{-/-}$ mice had lower levels of transcripts for TGF-β1 (**A**) and OPN (**B**) compared with that seen in the lungs of vehicle-treated $ADA^{-/-}$ mice. *$P \leq 0.05$ versus ADA^+; #$P \leq 0.05$ versus vehicle-treated $ADA^{-/-}$. $n = 4$ (ADA^+), 8 (ADA^+). (**C–E**) Immunolocalization of TGF-β1. (**F–H**) Immunolocalization of OPN. Lung sections from vehicle-treated ADA^+ mice (**C** and **F**), vehicle-treated $ADA^{-/-}$ mice (**D** and **G**), and CVT-6883–treated $ADA^{-/-}$ mice (**E** and **H**) are shown. Arrows denote macrophages. Scale bars: 100 μm.

Increased collagen production and deposition are hallmarks of pulmonary fibrosis (30). Examination of collagen deposition using Masson's trichrome staining revealed that there was little to no collagen deposition in the lungs of ADA^+ vehicle- or CVT-6883–treated mice (Figure 7, D and E), whereas airway collagen deposition was prominent in vehicle-treated $ADA^{-/-}$ mice (Figure 7F). In contrast, treatment of $ADA^{-/-}$ mice with CVT-6883 resulted in a reduction in collagen deposition in the airways (Figure 7G). Collagen production was measured by quantifying whole-lung α1-procollagen transcript levels (Figure 7H) and collagen protein levels in BAL fluid (Figure 7I). Significant increases in collagen production were seen in the lungs of $ADA^{-/-}$ mice treated with vehicle, and these increases were largely prevented by CVT-6883 treatment. These findings demonstrate that CVT-6883 can inhibit the development of fibrosis in $ADA^{-/-}$ mice and implicate $A_{2B}AR$ signaling in the regulation of collagen deposition.

Reduction in profibrotic mediators in the lungs. TGF-β1 and osteopontin (OPN) are profibrotic mediators whose expression has been shown to be elevated in the lungs of $ADA^{-/-}$ mice (15). The levels of these fibrotic regulators were increased in the lungs of $ADA^{-/-}$ mice treated with vehicle, while CVT-6883 treatment decreased expression of these molecules (Figure 8, A and B). Immunolocalization studies revealed that increases in TGF-β1 (compare Figure 8, C and D) and OPN (compare Figure 8, F and G) in the lungs of $ADA^{-/-}$ mice were localized predominantly to alveolar macrophages. Furthermore, diminished TGF-β1 (Figure 8E) and OPN (Figure 8H) immunoreactivity in alveolar macrophages was seen following CVT-6883 treatment. These findings suggest that $A_{2B}AR$ antagonism can alter the expression of key regulators of fibrosis in macrophages found in the lungs of $ADA^{-/-}$ mice.

$A_{2B}AR$ expression and adenosine levels in the lungs of $ADA^{-/-}$ mice treated with CVT-6883. Alterations in

$A_{2B}AR$ expression have been noted in the lungs of $ADA^{-/-}$ mice (26, 31) and in the lungs of mice exhibiting Th2-driven pulmonary inflammation and damage (13). The levels of $A_{2B}AR$ transcripts were measured in whole-lung RNA extracts from ADA^+ and $ADA^{-/-}$ mice treated with vehicle or CVT-6883 to determine the consequence of antagonist treatment on receptor levels. $A_{2B}AR$ transcript levels were elevated in the lungs of $ADA^{-/-}$ mice treated with vehicle, and there was a significant reduction in the expression of receptors found in the lungs of $ADA^{-/-}$ mice treated with CVT-6883 (Figure 9A). As expected, lung adenosine levels were elevated in $ADA^{-/-}$ mice treated with vehicle (Figure 9B). Adenosine levels remained elevated in the lungs of $ADA^{-/-}$ mice treated with CVT-6883, although there was a trend toward decreased concentration (Figure 9B). These findings demonstrate that $A_{2B}AR$ and adenosine levels were elevated in the lungs of the $ADA^{-/-}$ mice used in this study and suggest that treatment with CVT-6883 can impact their levels.
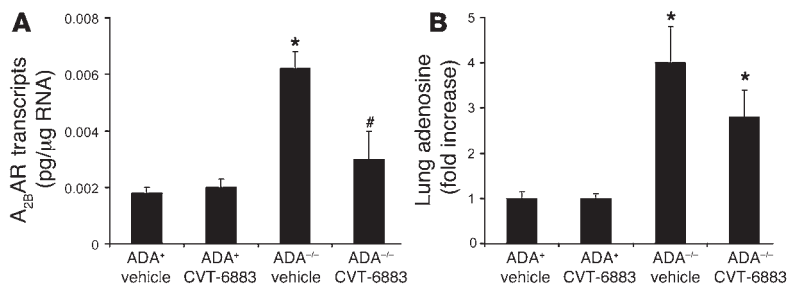
Figure 9
$A_{2B}AR$ transcript and adenosine levels in the lungs. (**A**) RNA was extracted from whole lungs of postnatal day 38 mice for analysis of $A_{2B}AR$ expression using quantitative RT-PCR. Data are mean transcript levels ± SEM. *$P \leq 0.05$ versus vehicle-treated ADA^+; #$P \leq 0.05$ versus vehicle-treated $ADA^{-/-}$. $n = 4$ (ADA^+), 8 ($ADA^{-/-}$). (**B**) Adenine nucleotides were extracted from whole lungs of postnatal day 38 mice, and adenosine levels were quantified by reverse-phase HPLC. Data are mean fold increase ± SEM. *$P \leq 0.05$ versus ADA^+. $n = 4$ per group.
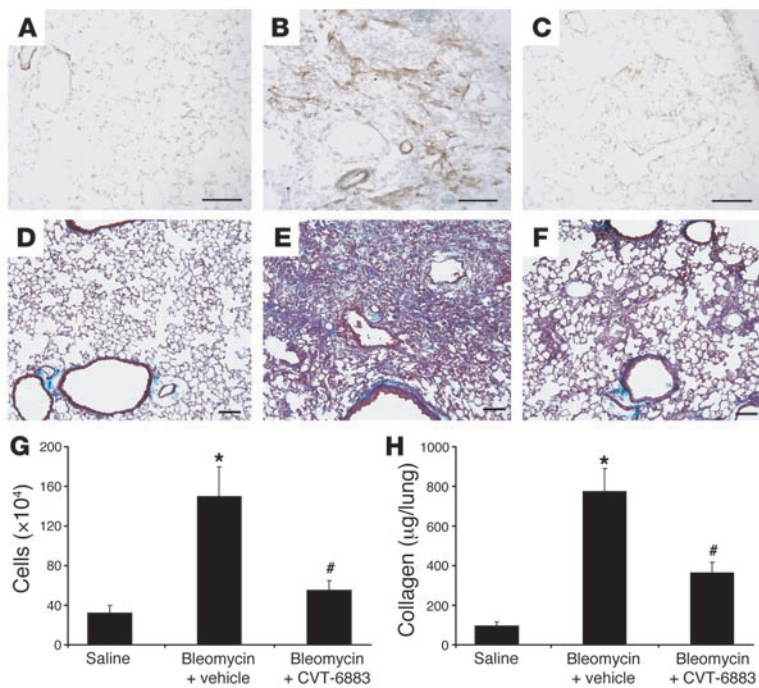
Figure 10
CVT-6883 treatment in a model of bleomycin-induced pulmonary injury. (**A–C**) Lung sections were stained with an antibody against α-SMA to visualize myofibroblast (brown). (**D–F**) Lung sections were stained with Masson's trichrome to visualize collagen (blue). Shown are lungs from saline-treated mice 14 days after treatment (**A** and **D**) and bleomycin-treated mice 14 days after treatment that were treated with vehicle (**B** and **E**) or CVT-6883 (**C** and **F**) beginning on day 5 of the protocol. Sections are representative of 7 different mice from each treatment. Scale bars: 100 μm. (**G**) Total BAL cells. Data are mean ± SEM. (**H**) Whole-lung collagen protein levels. Data are mean μg collagen/lung ± SEM. *$P \leq 0.05$ versus saline-treated mice; #$P \leq 0.05$ versus vehicle-treated bleomycin-exposed mice. $n = 7$ per group.

CVT-6883 treatment is associated with a reduction in bleomycin-induced pulmonary fibrosis. Recent work from our laboratory has demonstrated that adenosine levels are increased in the lungs of mice exhibiting bleomycin-induced pulmonary fibrosis (32). To determine the consequence of $A_{2B}AR$ antagonism in this model, 8-week-old C57BLk/6J female mice were treated intratracheally with 3.0 U/kg bleomycin and then treated with either vehicle or CVT-6883. Mice treated with bleomycin in conjunction with vehicle had increased myofibroblast differentiation (compare Figure 10, A and B), collagen deposition (compare Figure 10, D and E), collagen production (Figure 10H), and inflammation (Figure 10G), which was largely monocytic in nature (data not shown). Treatment of mice with bleomycin followed by CVT-6883 resulted in decreased levels of pulmonary fibrosis (Figure 10, C, F, and H) and inflammation (Figure 10G). These data demonstrate that CVT-6883 can attenuate pulmonary inflammation and fibrosis in bleomycin-induced lung injury.

Discussion

Adenosine activates both antiinflammatory (tissue-protective) and proinflammatory (tissue-destructive) pathways (12, 33). The various actions of adenosine are likely dependent on the type and duration of injury, the amount of adenosine produced, the cytokine milieu, and the expression of the subtypes of ARs. The $ADA^{-/-}$ mouse model of adenosine-dependent pulmonary injury has provided in vivo evidence that prolonged increases in adenosine levels can directly promote aspects of pulmonary inflammation, airway remodeling, and pulmonary tissue destruction (14–16). However, the AR subtypes involved have not yet been established. The $A_{2B}AR$ is widely expressed in tissues and cells and has the lowest affinity for adenosine (20, 21). This feature has led to the hypothesis that activation of the $A_{2B}AR$ may be important in situations where adenosine levels are increased, such as following tissue hypoxia or inflammation. However, the function of $A_{2B}AR$

activation in vivo has not been well characterized due to the lack of selective pharmacological agents or genetic models that allow the study of their function in the whole animal. The current study used the $ADA^{-/-}$ model system to uncover what we believe to be novel and important aspects of adenosine-mediated lung injury that are mediated by the $A_{2B}AR$. Adenosine levels accumulate to concentrations as high as 100 μM in the lungs of $ADA^{-/-}$ mice in association with increased lung inflammation and injury, making it an ideal model system for examining potential involvement of the low-affinity $A_{2B}AR$. Treatment of $ADA^{-/-}$ mice with the novel selective $A_{2B}AR$ antagonist CVT-6883 was able to markedly reduce pulmonary inflammation, fibrosis, and airspace enlargement. These findings suggest that $A_{2B}AR$ signaling is a major contributor to lung injury in environments where endogenous adenosine levels are elevated. These findings were not unique to the $ADA^{-/-}$ model, as CVT-6883 treatment also attenuated pulmonary inflammation and fibrosis in wild-type mice treated with bleomycin. These findings may have implications for the treatment of various chronic lung diseases including asthma, COPD, and pulmonary fibrosis.

A major observation in this study was that CVT-6883 treatment reduced the number of inflammatory cells recovered in the BAL fluid of $ADA^{-/-}$ mice. There were reductions in lymphocytes, neutrophils, eosinophils, and alveolar macrophages. In addition, there was a reduction in the production of cytokines and chemokines in the lungs of these mice, suggesting that $A_{2B}AR$ signaling may contribute to pulmonary inflammation through increased production of these mediators. $A_{2B}AR$ antagonism also diminished the apparent activation of alveolar macrophages. The macrophages recovered from the BAL fluid of vehicle-treated $ADA^{-/-}$ mice were enlarged and foamy, whereas there were few to no foam cells observed in the BAL from $ADA^{-/-}$ mice treated with CVT-6883, which suggests that blocking $A_{2B}AR$ can prevent the activation of alveolar macrophages. Alveolar macrophages express the $A_{2B}AR$ (13), and evidence exists to suggest that the expression of $A_{2B}AR$ is increased in activated mac-

rophages (34). Thus $A_{2B}AR$ signaling in alveolar macrophages may directly regulate the activation of macrophages and/or the production of key mediators by these cells. Consistent with this, there was diminished expression of macrophage-derived mediators such as IL-6, OPN, TGF-β1, and MMPs in the lungs of $ADA^{-/-}$ mice treated with CVT-6883. The expression of these mediators by activated macrophages can contribute to airway remodeling and destruction (5). The ability of CVT-6883 to reduce the degree of fibrosis and enlargement of airspaces seen in $ADA^{-/-}$ mice may therefore be related to the production of mediators by macrophages. It is also likely that $A_{2B}AR$ signaling on other cell types including airway epithelial cells (13), smooth muscle cells (23), and fibroblasts (22) also play a significant role in this model.

Another prominent feature of adenosine-induced lung injury in $ADA^{-/-}$ mice is the destruction of alveolar airspaces, a response reminiscent of emphysema (16, 35). Treatment of $ADA^{-/-}$ mice with CVT-6883 prevented airspace enlargement, suggesting that $A_{2B}AR$ signaling plays an important role in the emphysemic phenotype of this model. Protease/antiprotease imbalances are thought to mediate alveolar wall destruction that can lead to enlarged airspaces (2, 5). Consistent with this, there is a prominent increase in the production of proteases and antiproteases in the lungs of $ADA^{-/-}$ mice (16). The current study demonstrated that antagonism of the $A_{2B}AR$ in vivo can reduce elevations in the expression of MMP-9, MMP-12, and TIMP-1 in the lungs of $ADA^{-/-}$ mice, suggesting that $A_{2B}AR$ is involved in the regulation of protease and antiprotease levels. Interestingly, opposite effects were seen when A_1AR signaling was blocked in the lungs of $ADA^{-/-}$ mice (16). Genetic removal of the high-affinity A_1AR from $ADA^{-/-}$ mice resulted in an enhancement of macrophage accumulation, MMP expression, and airspace enlargement, suggesting that the A_1AR serves antiinflammatory, tissue-protective roles in the $ADA^{-/-}$ model. Thus the A_1AR and the $A_{2B}AR$ appear to have opposing actions on chronic aspects of adenosine-induced lung injury. This may be due to the fact that these receptor subtypes couple to different intracellular signaling pathways (17, 21).

Inflammation and repair are normal processes that follow tissue injury. However, when injury is excessive or repetitive, repair processes result in tissue fibrosis. Fibrosis is characterized by the accumulation of myofibroblasts that express α-SMA, the deposition of extracellular matrix molecules such as collagen, and the distortion of normal tissue architecture, which, in the case of pulmonary fibrosis, leads to the loss of gas exchange and normal lung function (30). Pulmonary fibrosis is a prominent feature in $ADA^{-/-}$ mice, in which increases in lung adenosine levels have been attributed to the activation of profibrotic pathways that culminate in myofibroblast proliferation and excessive collagen production (15, 31). Findings in the current study suggest that signaling through the $A_{2B}AR$ is responsible for the adenosine-dependent fibrotic changes seen in this model. Blocking $A_{2B}AR$ signaling using CVT-6883 prevented myofibroblast proliferation and subsequent collagen production and deposition in the lungs of $ADA^{-/-}$ mice. This feature is not unique to fibrosis in the $ADA^{-/-}$ model, as CVT-6883 was also able to reduce myofibroblast proliferation and collagen deposition in wild-type mice challenged with bleomycin. Together, these findings suggest that $A_{2B}AR$ signaling contributes to the development of pulmonary fibrosis. Supporting these findings is a recent study in human pulmonary fibroblasts cultured in vitro, where it was demonstrated that activation of the $A_{2B}AR$ can promote the differentiation of pulmonary fibroblasts into α-SMA–positive myofibroblasts (22). This response involved the release of IL-6 and was enhanced in

the presence of hypoxia. Interestingly, the prevention of fibrosis in the lungs of CVT-6883–treated $ADA^{-/-}$ mice was also associated with decreased IL-6 production, suggesting that this profibrotic cytokine (36) may be a primary mediator involved in adenosine-induced pulmonary fibrosis. Other prominent mediators of fibrosis whose expression is increased in the lungs of $ADA^{-/-}$ mice and reduced upon CVT-6883 treatment include TGF-β1 and OPN. Unlike IL-6, adenosine has not been shown to directly regulate these mediators in other systems. It is therefore not possible to discern from these studies whether adenosine signaling through the $A_{2B}AR$ is directly or indirectly responsible for the increases in TGF-β1 and OPN in the lungs of $ADA^{-/-}$ mice. However, our studies do demonstrate that alveolar macrophages are a prominent source of $A_{2B}AR$-dependent expression of these profibrotic mediators.

The transformation of pulmonary fibroblasts into myofibroblasts is considered a major mechanism underlying pulmonary fibrosis (3, 37). The demonstration that activation of the $A_{2B}AR$ can promote these processes (22) further supports the hypothesis that adenosine is in itself profibrotic and strongly implicates the $A_{2B}AR$ as a mediator of the profibrotic response. However, it must be noted that other studies have implicated adenosine, acting through the $A_{2B}AR$, as an antifibrotic signal via its ability to inhibit cardiac fibroblast growth and collagen production (38, 39). Interestingly, in one of these studies, activation of the $A_{2B}AR$ with high levels of agonist actually promoted collagen production (39), suggesting that there may be a threshold for the antifibrotic effects of $A_{2B}AR$ signaling in cardiac fibroblasts.

The $A_{2B}AR$ largely couples to $G_{\alpha s}$ to stimulate adenylate cyclase and elevate cAMP levels (21). In addition, evidence exists to suggest the $A_{2B}AR$ can couple to $G_{\alpha q}$, which can affect intracellular Ca^{2+} levels (40, 41). Recent studies have drawn attention to the ability of the $A_{2B}AR$ to activate MAPK pathways including p38, ERK1/2, and JNK (42, 43). These intracellular signaling pathways play an essential role in processes such as cell differentiation, proliferation, survival, and apoptosis (44). Moreover, they can regulate the production of cytokines and proteases in the lung, including IL-6 and MMP-9 (45, 46), and appear to play an important role in mediating features of pulmonary fibrosis including collagen deposition and profibrotic mediator regulation (47). It is therefore possible that activation of MAPK signaling pathways by the $A_{2B}AR$ may underlie the adenosine-mediated effects seen in chronic lung injury. More studies are needed to directly define the role of these pathways in these processes.

In conclusion, the results of the present study demonstrated that antagonism of the $A_{2B}AR$ inhibits pulmonary inflammation and injury in the lungs of $ADA^{-/-}$ mice and in a model of bleomycin-induced lung injury. These findings are consistent with the hypothesis that $A_{2B}AR$ signaling contributes to the proinflammatory and profibrotic activities present in chronic lung diseases. Additional studies are needed to extend these observations to other models of chronic lung diseases and to humans. Nevertheless, this study represents the first in vivo preclinical evidence to our knowledge that $A_{2B}AR$ antagonism may be of significant therapeutic value to the management of chronic lung diseases such as severe asthma, COPD, and pulmonary fibrosis.

Methods

CVT-6883 receptor binding assays and cAMP assays. CVT-6883 (Figure 1A) was synthesized by the Department of Bio-Organic Chemistry at CV Therapeutics Inc. Human cDNAs for $A_{2A}AR$, $A_{2B}AR$, and A_3AR were cloned

into expression vectors and transfected into HEK-293 or CHO cells using Lipofectin-Plus (Invitrogen). CHO cells overexpressing the human A_1AR were obtained from J. Shryock (University of Florida, Gainesville, Florida, USA). Cells were harvested in a buffer containing 10 mM HEPES (pH 7.4), 10 mM EDTA, and protease inhibitor cocktail (Roche Diagnostics), and homogenates were centrifuged at 29,000 g for 15 minutes at 4°C. Cell pellets were washed with a buffer containing 10 mM HEPES (pH 7.4), 1 mM EDTA, and protease inhibitors and were resuspended in buffer containing 10% sucrose. The affinity of CVT-6883 for the various ARs was determined in competition studies using the following radioligands (17, 48): ^{3}H-CPX (A_1AR antagonist; 0.45 nM), ^{3}H-ZM241385 ($A_{2A}AR$ antagonist; 1.6 nM), ^{3}H-ZM241385 ($A_{2B}AR$ antagonist; 9.3 nM), and ^{3}H-MRE3008F20 (A_3AR antagonist; 0.63 nM). Radioligands were mixed with increasing concentrations of CVT-6883 and 20 μg membrane proteins in 50 mM Tris and 1 mM EDTA containing 1 U/ml ADA. The assays were incubated for 60–90 minutes, stopped by filtration onto GF/B filter plates, and washed 4 times with ice-cold TM buffer (10 mM Tris, 1 mM $MgCl_2$, pH 7.4), after which bound ligand was determined by scintillation counting. Nonspecific binding was determined in the presence of 1–10 μM ligands.

For cAMP determinations, suspensions of NIH/3T3 at a concentration of 0.5×10^6 cells/ml were incubated with 1 U/ml ADA for 30 minutes at room temperature. Cell suspensions were then treated with increasing concentrations of NECA in the absence or presence of CVT-6883 for 15 minutes at 37°C. Rolipram (50 μM), a phosphodiesterase inhibitor, was also present to inhibit the degradation of cAMP. After the incubation, cells were lysed, and cAMP concentrations were determined using cAMP-Screen Direct System (Applied Biosystems) according to the manufacturer's instructions.

Mice. ADA-deficient mice were generated and genotyped as described previously (19, 49). Mice homozygous for the null *Ada* allele were designated ADA deficient ($ADA^{-/-}$), while mice heterozygous for the null *Ada* allele were designated as ADA control mice (ADA^+). All mice were on a mixed 129sv/C57BL/6J background, and all phenotypic comparisons were performed among littermates. C57BLk/6J female mice for bleomycin studies were purchased from Harlan. Animal care was in accordance with institutional and NIH guidelines. These studies were reviewed and approved by the University of Texas Health Science Center at the Houston Animal Welfare Committee in Houston, Texas, USA. Mice were housed in ventilated cages equipped with microisolator lids and maintained under strict containment protocols. No evidence of bacterial, parasitic, or fungal infection was found, and serologies on cage littermates were negative for 12 of the most common murine viruses.

Antagonist treatment. $ADA^{-/-}$ mice were identified at birth by screening for ADA enzymatic activity in the blood as described previously (19). $ADA^{-/-}$ mice were maintained on ADA enzyme therapy from postnatal day 2 until postnatal day 21 (19). On postnatal day 24, treatments with CVT-6883 (1 mg/kg) or vehicle (corn oil/ethanol/DMSO) were initiated. Treatments consisted of an intraperitoneal injection in the morning and in the evening for 14 days. Treatment groups included $ADA^{-/-}$ or ADA^+ mice receiving CVT-6883, vehicle, or no treatment. All mice were littermates, and both males and females were included in these experiments. The same formulation and dose of CVT-6883 described above was used in bleomycin studies, where twice-daily intraperitoneal injections were given on days 5–14 of the protocol.

Bleomycin exposures. Six-week-old female C57BLk/6J mice were used. Mice were anesthetized with avertin, and 3.0 U/kg bleomycin (Blenoxane, Bristol-Myers Squibb) diluted in 50 μl normal saline, or 50 μl normal saline alone, was instilled intratracheally (32). End points were measured 14 days after challenge.

Cellular differentials and histology. Mice were anesthetized with avertin, lungs were lavaged 4 times with 0.5 ml PBS, and 1.5 ml of pooled lavage fluid was recovered. Total cell counts were determined using a hemocytometer, and

aliquots were cytospun onto microscope slides and stained with Diff-Quik (Dade Behring) for cellular differentials. Lungs were then infused with 4% paraformaldehyde in PBS at 25 cm H_2O pressure and fixed overnight at 4°C. Fixed lung samples were rinsed in PBS, dehydrated, and embedded in paraffin. Sections (5 μm) were collected on microscope slides and stained with H&E (Thermo Electron Corp.) or Masson's trichrome (EM Science) according to the manufacturers' instructions.

Analysis of mRNA. Mice were anesthetized, and the lungs were rapidly removed and frozen in liquid nitrogen. RNA was isolated from frozen lung tissue using TRIZOL reagent (Invitrogen). RNA samples were then DNase treated and subjected to quantitative real-time RT-PCR. The primers, probes, and procedures for real-time RT-PCR were described previously (16). Reactions were carried out on a SmartCycler System (Cepheid). Specific transcript levels were determined using SmartCycler Software (version 4.0; Cepheid) through comparison to a standard curve generated from the PCR amplification of template dilutions.

Determination of alveolar airspace size. The size of alveolar airways was determined in pressure-infused lungs by measuring mean chord lengths on H&E-stained lung sections (14). Representative images were digitized, and a grid consisting of 53 black lines at 10.5-μm intervals was overlaid on the image. This line grid was subtracted from the lung images using Image-Pro Plus image analysis software (version 2.0; MediaCybernetics), and the resultant lines were measured and averaged to give the mean chord length of the alveolar airways. The final mean chord lengths represent averages from 10 nonoverlapping images of each lung specimen. All quantitative studies were performed blinded with regard to animal genotype.

Collagen quantification. The Sircol Collagen Assay (Biocolor Assays) to measure soluble collagen was performed on BAL fluid or whole-lung extracts according to the manufacturer's instructions.

Immunohistochemistry. Immunohistochemistry was performed on 5-μm sections cut from formalin-fixed, paraffin-embedded lungs. Sections were rehydrated through graded ethanols to water, endogenous peroxidases were quenched with 3% hydrogen peroxide, antigen retrieval was performed (Dako), and endogenous avidin and biotin was blocked with the Biotin-Blocking System (Dako). For α-SMA staining, slides were processed with the Mouse on Mouse Kit and the Elite Vectastain ABC Kit (Vector Laboratories) and incubated with a 1:500 dilution of a α-SMA monoclonal antibody (monoclonal clone 1 A-4; Sigma-Aldrich) overnight at 4°C. For TGF-β1 staining, a 1:200 dilution of polyclonal rabbit anti-mouse TGF-β1 antiserum (Santa Cruz Biotechnology Inc.) was used as described above; for OPN detection, polyclonal goat anti-mouse OPN antiserum (R&D Systems Inc.) at a concentration of 1:100 was used. Sections were developed with 3,3′-diaminobenzidine (Sigma-Aldrich) and counterstained with methyl green or hematoxylin.

Quantification of lung adenosine levels. Mice were anesthetized, and their lungs were rapidly removed and frozen in liquid nitrogen. Adenine nucleosides were extracted from frozen lungs using 0.4 P M perchloric acid as described previously (49), and adenosine was separated and quantified using reverse-phase HPLC.

Statistics. Values are expressed as mean ± SEM. As appropriate, groups were compared by analysis of variance; follow-up comparisons between groups were conducted using 2-tailed Student's t test. A P value of ≤0.05 was considered to be significant.

Acknowledgments

Address correspondence to: Michael R. Blackburn, Department of Biochemistry and Molecular Biology, University of Texas Medical School at Houston, Houston, Texas 77030, USA. Phone: (713) 500-6087; Fax: (713) 500-0652; E-mail: michael.r.blackburn@uth.tmc.edu.

1. Elias, J.A., et al. 2003. New insights into the pathogenesis of asthma. *J. Clin. Invest.* **111**:291–297. doi:10.1172/JCI200317748.
2. Senior, R.M., and Shapiro, S.D. 1998. Chronic obstructive pulmonary disease: epidemiology, pathophysiology, and pathogenesis. In *Fishman's pulmonary diseases and disorders*. A.P. Fishman, et al., editors. McGraw–Hill, Inc. New York, New York, USA. 659–681.
3. Thannickal, V.J., Toews, G.B., White, E.S., Lynch, J.P., 3rd, and Martinez, F.J. 2004. Mechanisms of pulmonary fibrosis. *Annu. Rev. Med.* **55**:395–417.
4. Bradding, P., Redington, A.E., and Holgate, S.T. 1997. Airway wall remodelling in the pathogenesis of asthma: cytokine expression in the airways. In *Airway wall remodelling in asthma*. A.G. Stewart, editor. CRC Press, Inc. Boca Raton, Florida, USA. 29–63.
5. Shapiro, S.D. 1999. The macrophage in chronic obstructive pulmonary disease. *Am. J. Respir. Crit. Care Med.* **160**:S29–S32.
6. Martin, C., Leone, M., Viviand, X., Ayem, M.L., and Guieu, R. 2000. High adenosine plasma concentration as a prognostic index for outcome in patients with septic shock. *Crit. Care Med.* **28**:3198–3202.
7. Sperlagh, B., Doda, M., Baranyi, M., and Hasko, G. 2000. Ischemic-like condition releases norepinephrine and purines from different sources in superfused rat spleen strips. *J. Neuroimmunol.* **111**:45–54.
8. Driver, A.G., Kukoly, C.A., Ali, S., and Mustafa, S.J. 1993. Adenosine in bronchoalveolar lavage fluid in asthma. *Am. Rev. Respir. Dis.* **148**:91–97.
9. Huszar, E., et al. 2002. Adenosine in exhaled breath condensate in healthy volunteers and in patients with asthma. *Eur. Respir. J.* **20**:1393–1398.
10. Day, Y.J., et al. 2004. Protection from ischemic liver injury by activation of A2A adenosine receptors during reperfusion: inhibition of chemokine induction. *Am. J. Physiol. Gastrointest. Liver Physiol.* **286**:G285–G293.
11. Ohta, A., and Sitkovsky, M. 2001. Role of G-protein-coupled adenosine receptors in downregulation of inflammation and protection from tissue damage. *Nature.* **414**:916–920.
12. Blackburn, M.R. 2003. Too much of a good thing: adenosine overload in adenosine-deaminase-deficient mice. *Trends Pharmacol. Sci.* **24**:66–70.
13. Blackburn, M.R., et al. 2003. Adenosine mediates IL-13-induced inflammation and remodeling in the lung: evidence for an IL-13-adenosine amplification pathway. *J. Clin. Invest.* **112**:332–344. doi:10.1172/JCI200316815.
14. Blackburn, M.R., et al. 2000. Metabolic consequences of adenosine deaminase deficiency in mice are associated with defects in alveogenesis, pulmonary inflammation, and airway obstruction. *J. Exp. Med.* **192**:159–170.
15. Chunn, J.L., et al. 2005. Adenosine-dependent pulmonary fibrosis in adenosine deaminase-deficient mice. *J. Immunol.* **175**:1937–1946.
16. Sun, C.X., et al. 2005. A protective role for the A(1) adenosine receptor in adenosine-dependent pulmonary injury. *J. Clin. Invest.* **115**:35–43. doi:10.1172/JCI200522656.
17. Fredholm, B.B., IJzerman, A.P., Jacobson, K.A., Klotz, K.N., and Linden, J. 2001. International Union of Pharmacology. XXV. Nomenclature and classification of adenosine receptors. *Pharmacol. Rev.* **53**:527–552.
18. Zhong, H., et al. 2003. Activation of murine lung mast cells by the adenosine A3 receptor. *J. Immunol.* **170**:338–345.
19. Young, H.W., et al. 2004. A3 adenosine receptor signaling contributes to airway inflammation and mucus production in adenosine deaminase-deficient mice. *J. Immunol.* **173**:1380–1389.
20. Beukers, M.W., den Dulk, H., van Tilburg, E.W., Brouwer, J., and Ijzerman, A.P. 2000. Why are A(2B) receptors low-affinity adenosine receptors? Mutation of Asn273 to Tyr increases affinity of human A(2B) receptor for 2-(1-Hexynyl)adenosine. *Mol. Pharmacol.* **58**:1349–1356.
21. Feoktistov, I., and Biaggioni, I. 1997. Adenosine A2B receptors. *Pharmacol. Rev.* **49**:381–402.
22. Zhong, H., Belardinelli, L., Maa, T., and Zeng, D. 2005. Synergy between A2B adenosine receptors and hypoxia in activating human lung fibroblasts. *Am. J. Respir. Cell Mol. Biol.* **32**:2–8.
23. Zhong, H., et al. 2004. A(2B) adenosine receptors increase cytokine release by bronchial smooth muscle cells. *Am. J. Respir. Cell Mol. Biol.* **30**:118–125.
24. Ryzhov, S., et al. 2004. Adenosine-activated mast cells induce IgE synthesis by B lymphocytes: an A2B-mediated process involving Th2 cytokines IL-4 and IL-13 with implications for asthma. *J. Immunol.* **172**:7726–7733.
25. Feoktistov, I., and Biaggioni, I. 1995. Adenosine A2b receptors evoke interleukin-8 secretion in human mast cells. An enprofylline-sensitive mechanism with implications for asthma. *J. Clin. Invest.* **96**:1979–1986.
26. Chunn, J.L., Young, H.W., Banerjee, S.K., Colasurdo, G.N., and Blackburn, M.R. 2001. Adenosine-dependent airway inflammation and hyperresponsiveness in partially adenosine deaminase-deficient mice. *J. Immunol.* **167**:4676–4685.
27. Banerjee, S.K., Young, H.W., Barczak, A., Erle, D.J., and Blackburn, M.R. 2004. Abnormal alveolar development associated with elevated adenine nucleosides. *Am. J. Respir. Cell Mol. Biol.* **30**:38–50.
28. Hautamaki, R.D., Kobayashi, D.K., Senior, R.M., and Shapiro, S.D. 1997. Requirement for macrophage elastase for cigarette smoke-induced emphysema in mice. *Science.* **277**:2002–2004.
29. Lanone, S., et al. 2002. Overlapping and enzyme-specific contributions of matrix metalloproteinases-9 and -12 in IL-13-induced inflammation and remodeling. *J. Clin. Invest.* **110**:463–474. doi:10.1172/JCI200214136.
30. Lynch, J., and Toews, G. 1998. Idiopathic pulmonary fibrosis. In *Pulmonary diseases and disorders*. A.P. Fishman, et al., editors. McGraw–Hill. New York, New York, USA. 1069–1084.
31. Chunn, J.L., et al. 2006. Partially adenosine deaminase-deficient mice develop pulmonary fibrosis in association with adenosine elevations. *Am. J. Physiol. Lung Cell. Mol. Physiol.* **290**:L579–L587.
32. Volmer, J.B., Thompson, L.F., and Blackburn, M.R. 2006. Ecto-5′-nucleotidase (CD73)-mediated adenosine production is tissue protective in a model of bleomycin-induced lung injury. *J. Immunol.* **176**:4449–4458.
33. Linden, J. 2001. Molecular approach to adenosine receptors: receptor-mediated mechanisms of tissue protection. *Annu. Rev. Pharmacol. Toxicol.* **41**:775–787.
34. Xaus, J., et al. 1999. IFN-gamma up-regulates the A2B adenosine receptor expression in macrophages: a mechanism of macrophage deactivation. *J. Immunol.* **162**:3607–3614.
35. Blackburn, M.R., et al. 2000. The use of enzyme therapy to regulate the metabolic and phenotypic consequences of adenosine deaminase deficiency in mice. Differential impact on pulmonary and immunologic abnormalities. *J. Biol. Chem.* **275**:32114–32121.
36. Knight, D.A., Ernst, M., Anderson, G.P., Moodley, Y.P., and Mutsaers, S.E. 2003. The role of gp130/IL-6 cytokines in the development of pulmonary fibrosis: critical determinants of disease susceptibility and progression? *Pharmacol. Ther.* **99**:327–338.
37. King, T.E., Jr., et al. 2001. Idiopathic pulmonary fibrosis: relationship between histopathologic features and mortality. *Am. J. Respir. Crit. Care Med.* **164**:1025–1032.
38. Dubey, R.K., Gillespie, D.G., Zacharia, L.C., Mi, Z., and Jackson, E.K. 2001. A(2b) receptors mediate the antimitogenic effects of adenosine in cardiac fibroblasts. *Hypertension.* **37**:716–721.
39. Chen, Y., et al. 2004. Functional effects of enhancing or silencing adenosine A2b receptors in cardiac fibroblasts. *Am. J. Physiol. Heart Circ. Physiol.* **287**:H2478–H2486.
40. Gao, Z., Chen, T., Weber, M.J., and Linden, J. 1999. A2B adenosine and P2Y2 receptors stimulate mitogen-activated protein kinase in human embryonic kidney-293 cells. Cross-talk between cyclic AMP and protein kinase c pathways. *J. Biol. Chem.* **274**:5972–5980.
41. Linden, J., Thai, T., Figler, H., Jin, X., and Robeva, A.S. 1999. Characterization of human A(2B) adenosine receptors: radioligand binding, western blotting, and coupling to G(q) in human embryonic kidney 293 cells and HMC-1 mast cells. *Mol. Pharmacol.* **56**:705–713.
42. Feoktistov, I., Goldstein, A.E., and Biaggioni, I. 1999. Role of p38 mitogen-activated protein kinase and extracellular signal-regulated protein kinase kinase in adenosine A2B receptor-mediated interleukin-8 production in human mast cells. *Mol. Pharmacol.* **55**:726–734.
43. Schulte, G., and Fredholm, B.B. 2003. The G(s)-coupled adenosine A(2B) receptor recruits divergent pathways to regulate ERK1/2 and p38. *Exp. Cell Res.* **290**:168–176.
44. Schulte, G., and Fredholm, B.B. 2003. Signalling from adenosine receptors to mitogen-activated protein kinases. *Cell. Signal.* **15**:813–827.
45. Underwood, D.C., et al. 2000. SB 239063, a p38 MAPK inhibitor, reduces neutrophilia, inflammatory cytokines, MMP-9, and fibrosis in lung. *Am. J. Physiol. Lung Cell. Mol. Physiol.* **279**:L895–L902.
46. Carter, A.B., Monick, M.M., and Hunninghake, G.W. 1999. Both Erk and p38 kinases are necessary for cytokine gene transcription. *Am. J. Respir. Cell Mol. Biol.* **20**:751–758.
47. Matsuoka, H., et al. 2002. A p38 MAPK inhibitor, FR-167653, ameliorates murine bleomycin-induced pulmonary fibrosis. *Am. J. Physiol. Lung Cell. Mol. Physiol.* **283**:L103–L112.
48. Varani, K., et al. 2000. [(3)H]MRE 3008F20: a novel antagonist radioligand for the pharmacological and biochemical characterization of human A(3) adenosine receptors. *Mol. Pharmacol.* **57**:968–975.
49. Blackburn, M.R., Datta, S.K., and Kellems, R.E. 1998. Adenosine deaminase-deficient mice generated using a two-stage genetic engineering strategy exhibit a combined immunodeficiency. *J. Biol. Chem.* **273**:5093–5100.